The Influence of the Substituting Element (M = Ca, Sr, Ba) in $La_{1.7}M_{0.3}NiO_{4+\delta}$ on the Electrochemical Performance of the Composite Electrodes

E.Yu. Pikalova[1,2*] and A.A. Kolchugin[1]

[1]Institute of High Temperature Electrochemistry, 20 Academicheskaya str., 620137, Yekaterinburg, GSP-16, Russia
[2]Ural Federal University, 19 Mira str., 620002, Yekaterinburg, Russia

Article info

Received:
26August 2015

Received and revised form:
20 October 2015

Accepted:
30 November 2015

Abstract

The actual work focuses on the development of electrochemically active and stable electrodes for a high temperature proton-conducting electrolyte with a perspective of application in intermediate temperature electrochemical devices. The comparative study of the electrochemical performance of the $La_{1.7}M_{0.3}NiO_{4+\delta}$ – based (M = Ca, Sr, Ba) composite cathodes with proton-conducting $BaCe_{0.89}Gd_{0.1}Cu_{0.01}O_3$ or oxygen-ion-conducting $Ce_{0.8}Sm_{0.2}O_{1.9}$ ceramic components in contact with the proton-conducting electrolyte $BaCe_{0.89}Gd_{0.1}Cu_{0.01}O_3$ was performed by an impedance spectroscopy in wet air during 1500 h. The composites were used as functional layers in bi-layered electrodes with current collector layers made of 98 wt.% $LaNi_{0.6}Fe_{0.4}O_3$ + 2 wt.% CuO or 99.4 wt.% $La_{0.6}Sr_{0.4}MnO_3$ + 0.6 wt.% CuO.

1. Introduction

High temperature proton-conducting oxide materials are of great fundamental and practical interest because of the phenomenon of proton conductivity which appears along with oxygen-ionic conductivity when placed in a humidified atmosphere [1, 2]. Usage of such co-ionic electrolyte materials in solid oxide fuel cells (SOFCs) will give increased efficiency as a result of the higher open circuit voltage value and, correspondingly, the higher power output compared with SOFCs based on unipolar oxygen-ion-conducting electrolytes [3, 4]. Among high temperature proton conductors, $BaCeO_3$ doped with acceptor dopants (such as Gd, Sm, Y) demonstrates the highest co-ionic conductivity [5, 6]. $BaCeO_3$-based materials, despite some difficulties with their practical application because of weak chemical stability in the presence of salt-forming gas components (such as CO_2, H_2S, SO_2), could be the ideal electrolytes to be used in the pure hydrogen-fed SOFCs and other electrochemical devices such as electrolyzers, hydrogen and combustible gas sensors etc [1, 7].

The new electrolyte materials require well matched and electrochemically active electrode materials. The first studies concerning SOFCs based on $BaCe(Zr)O_3$ reported the use of a platinum cathode [7]. However, Pt is not preferred for practical applications due to its high cost. Moreover, the Pt electrodes were found to show significant polarization losses caused by the limited number of reaction sites at the cathode/electrolyte interface. From this viewpoint, cathode materials with mixed oxygen- ionic and electronic conductivity widely used in SOFCs on the base of unipolar oxygen-ion conductors (such as stabilized ZrO_2, doped CeO_2, doped $LaGaO_3$) so far as their application permits to broaden significantly a zone of electrochemical reaction [8], can be also applied in SOFCs with co-ionic conductors. However the development of an electrode material with proton conductivity would still be preferable since such cathodes allow the simultaneous transport of ionic (proton, oxygen-ion) and electronic defects under typical fuel cell operating conditions, thus offering to extend the electrochemically active area and correspondingly, decrease the polarization losses [9]. Additionally, electrode materials must be thermodynamically stable under working conditions: 400–900 °C, $10^{-5} < pO_2/atm \leq 0.21$, in the presence of H_2O and CO_2. Thermal affinity between electrolyte and cathode materials should be considered in order to attain both long-term stability and cycling.

* Corresponding author. E-mail: e.pikalova@list.ru

Over the past 10 years the layered nickelate $La_2NiO_{4+\delta}$ (LNO) with the coefficient of thermal expansion (CTE) α equal to 12.9–13.5 × 10^{-6} K^{-1}, high value of the oxygen surface heteroexchange constant k (2.5 × 10^{-6} cm s^{-1} at 800 °C) and oxygen diffusion coefficient D (1.7 × 10^{-7} cm^2 s^{-1} at 800 °C) [10] has been the subject of intensive studies including its application in an SOFC with proton conducting electrolytes [11–14]. As far as $La_2NiO_{4+\delta}$ is a *p*-type conductor in the temperature range 400–900 °C, appropriate acceptor doping in A-site could improve its electronic conductivity by generating extra electron holes for charge compensation. Experimental results reveal that doping with a certain amount of alkaline-earth metals (Ca, Sr. Ba) leads to an increase in total conductivity of substituted $La_2NiO_{4+\delta}$ [15–17]. It has been found that $LnNiO_{4+\delta}$ (Ln = Pr, Nd) substituted by Ca and Sr show better cathodic properties than the undoped materials [18–20]. But there are few studies dealing with the electrochemical properties of substituted $La_2NiO_{4+\delta}$. In our previous work on the development of the cathodes for $Ce_{0.8}Sm_{0.2}O_{1.9}$ electrolyte we showed that despite having increased conductivity, Sr and Ca-substituted $La_2NiO_{4+\delta}$ possessed lower polarization conductivity in comparison with the undoped one [17, 21]. We found that one possible way to increase the electrochemical performance was to use the composite materials with an ionic conductor in their composition, preferably of the same chemical composition as the electrolyte support, as a functional layer. In the case of a proton conducting electrolyte support a proton conducting ceramic in the composite electrode material would be preferable in terms of broadening the zone of electrochemical reaction and having a better match in CTE with the electrolyte.

The actual work focuses on the comparative study of the electrochemical performance of the $La_{1.7}M_{0.3}NiO_{4+\delta}$ – based bi-layered electrodes (M = Ca, Sr, Ba) in contact with the proton-conducting electrolyte $BaCe_{0.89}Gd_{0.1}Cu_{0.01}O_3$. The electrolyte material was selected because of its superior densification at low sintering temperatures and high proton conductivity [2, 6, 22]. The composites based on $La_{1.7}M_{0.3}NiO_{4+\delta}$ were made using $BaCe_{0.89}Gd_{0.1}Cu_{0.01}O_3$ ceramic component in their composition (50:50 wt.%) to ensure a partial proton conductivity in the electrode material and, for comparison, with oxygen ion conducting ceramic component $Ce_{0.8}Sm_{0.2}O_{1.9}$. The composites were used as functional layers in bi-layered electrodes. The current collector layers were made of 98 wt.% $LaNi_{0.6}Fe_{0.4}O_{3+2}$ wt.% CuO or 99.4 wt.% $La_{0.6}Sr_{0.4}MnO_3$ + 0.6 wt.% CuO, which were used before with the electrodes based on layered nickelates in contact with $Ce_{0.8}Sm_{0.2}O_{1.9}$ electrolyte [17, 23]. The performance of the electrodes and their long-term stability during 1500 h were investigated by impedance spectroscopy in wet air (5% H_2O).

2. Experimental

$La_{1.7}M_{0.3}NiO_{4+\delta}$ (M = Ca (LCNO), Sr (LSNO) and Ba (LBNO)), $LaNi_{0.6}Fe_{0.4}O_3$ (LNF) and $La_{0.6}Sr_{0.4}MnO_3$ (LSM) were synthesized via a two-step ceramic technology from the reagents with a purity of no less than 99.96%. The initial components were mixed in a planetary mill in isopropyl alcohol media using steel balls for 1 h, dried and calcined at 1150 °C for 2 h. The intermediate product underwent additional milling for 0.5 h followed by final synthesis at 1250 °C for 5 h. After final sintering, the powders were ball-milled up to the specific surface area equal to 1.5–2 m^2/g (SORBI N.4.1 analyzer).

The electrolytes $BaCe_{0.89}Gd_{0.1}Cu_{0.01}O_3$ (BCGCu) and $Ce_{0.8}Sm_{0.2}O_{1.9}$ (SDC) were synthesized using ceramic technology. After mixing, the initial components were calcined for 2 h at 1100 and 1050 °C, respectively, and ball-milled. The intermediate products were dry-pressed into disks at 150 MPa. The disks were then sintered at 1400 °C (BCGCu) and 1550 °C (SDC) for 5 h. Density of BCGCu and SDC electrolyte disks, determined from their geometrical dimensions and weights, was equal to 93–95% of the crystallographic values. XRD analysis of the powdered samples was performed by DMAX-2500, Rigaku Co. Ltd. diffractometer using Ni-filtered Cu Kα radiation in the range of $15 \leq 2\theta \leq 85°$. The thermal expansion of the materials was carried out using a Tesatronic TT-80 dilatometer between the room temperature and 900 °C with a heating/cooling rate of 3 °C min^{-1} in air. The average values of the coefficient of thermal expansion CTE were calculated on the linear section of dilatometric data.

To prepare the composite electrode materials the electrolyte disks were ground up to no less than 2.5 m^2/g and mixed with the electrode powders in 1:1 weight proportion with the addition of alcohol and a polyvinylbutyral organic binder. The electrodes were sited symmetrically on the BCGCu electrolyte substrates with the electrode surface area S equal to 0.25–0.36 cm^2 in the form of bi-layered coatings by brush-painting. The functional layers LCNO-BCGCu, LCNO-SDC, LSNO-BCGCu, LSNO-SDC, LBNO-BCGCu and LBNO-SDC

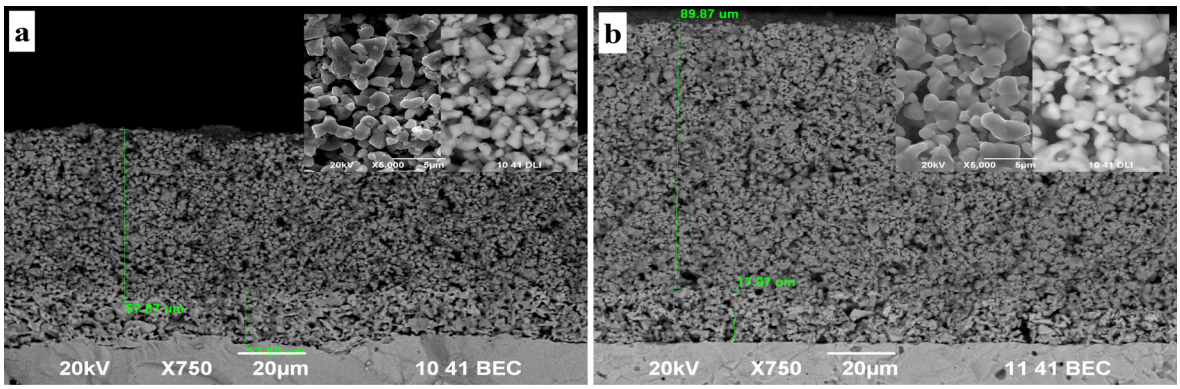

Fig. 1. Cross-sectional view of the bi-layered electrodes on the BCGCu electrolyte: (a) LCNO-SDC/LNF; (b) LCNO-BCGCu/LSM; surface structure of the LNF and LSM collector layers is shown in boxes. The porosity of functional and collector layers was approximately 35 and 50%, respectively.

were sintered at 1200 °C. After sintering, the thickness of the functional layers was about 20–25 μm. The collector layer was sited onto the pre-sintered functional layers. The sintering temperatures of the collector layers were 1050 and 1160 °C for LNF + 2 wt.% CuO and LSM + 0.6 wt.% CuO, respectively. The thickness of the collector layers was 50–90 μm to ensure a lower in-plane resistance of the electrodes, which is in a high importance for the electrodes in terms of practical application. The electrode morphology was characterized by scanning electron microscope JSM-5900LV (JEOL). Examples of bi-layer electrodes are presented in Fig. 1.

The electrochemical study was carried out using FRA-1260 with EI-1287 (Solartron Instruments Inc.). Up to six test samples were placed into a measuring cell. Each of them was pressed between two platinum current collecting nets with a thickness of 0.01 cm and a mesh size of 0.1 × 0.1 cm, which were connected to the measuring equipment by means of Pt wires via a two-electrode four-cable mode that permits the exclusion of the impedance of current-supplying cables from the overall impedance of the system. Measurements were performed in the temperature range 550–850 °C in wet air (5% H_2O) in the frequency range of 0.01 Hz to 100 kHz at the amplitude of applied sinusoidal signal of 20 mV. Each measurement was finished by measuring a full *dc* resistance R_{dc} of the cell.

The polarization resistance (R_η) of the electrochemical cell with symmetrically arranged electrodes was calculated as follows:

$$R_\eta = \frac{(R_{dc} - R_{hf})S}{2}, \quad (1)$$

where S is an electrode surface area, R_{dc} is a *dc* resistance of the electrochemical cell, and R_{hf} is a serial resistance determined by extrapolation of the high-frequency region of an impedance spectrum to the intersection with the x-axis and related to the electrolyte resistance, contact electrolyte-electrode resistance and a part of lateral resistance of the electrode.

The long-term study on the samples with bi-layered electrodes was performed at 700 °C during 1500 h. The test samples with single-layered electrodes without collector were subjected to the same conditions and after holding for 1000 h were retrieved for XRD testing. At 500 and 1000 h of testing the samples were cooled down to room temperature and heated again.

3. Results and Discussion

According to XRD (Table 1), the individual electrode materials were single-phase with a tetragonal (LCNO, LSNO, LBNO), hexagonal (LNF) and rhombohedrally distorted perovskite (LSM) structure. The electrolyte materials (XRD analyses were performed after high-temperature sintering at 1400 and 1550 °C for BCGCu and SDC, respectively) were characterized by a perovskite structure for proton conducting BCGCu electrolyte and by a fluorite structure in the case of oxygen ion conducting SDC.

LCNO, LSNO and LBNO in combination with both BCGCu and SDC ceramic component demonstrated good adhesion to the BCGCu electrolyte after sintering at 1200 °C. XRD analysis of the sintered functional layers revealed the appearance of some secondary phases (Table 2). Chemical interaction with SDC mainly consisted of a redistribution of the elements between perovskite and fluorite phases with the extraction of a trace amount of $Ce_{11}O_{20}$ and, in case of Ca-substituted nickelate, $Ce_{11}O_{20}$ and $LaNiO_3$. The degree of such

interaction is strongly dependent on the ionic radius of the rare earth element (REE) and it decreases with radius increasing (0.99, 1.12 and 1.34 Å for Ca, Sr and Ba). It is probably connected with a decrease in the solubility limit of the elements in a fluorite structure, which, as is known from the literature, is equal to 20, 8 and less than 2 mol.% for Ca, Sr and Ba, respectively [24]. Nevertheless, the interaction of substituted nickelates with SDC is remarkably lower than that in the case of undoped $La_2NiO_{4+\delta}$ [21]. The interaction in sintered composites with BCGCu was greater, except of Ba. The amount of the BaO extracted when evaluated from XRD data reached 4–6% in case of LCNO and 7–8% in case of LSNO, and in case of LBNO only trace amount of secondary phases was registered.

Table 1
Electrode and electrolyte powders characterization

Formula and designation	Space group	Parameters		
Electrode $La_{1.7}Ca_{0.3}NiO_{4+\delta}$(LCNO)	I4/mmm	a, Å 3.835	b, Å 3.835	c, Å 12.614
$La_{1.7}Sr_{0.3}NiO_{4+\delta}$(LSNO) $La_{1.7}Ba_{0.3}NiO_{4+\delta}$(LBNO)	I4/mmm I4/mmm	3.837 3.848	3.837 3.848	12.711 12.793
$LaNi_{0.6}Fe_{0.4}O_3$(LNF) $La_{0.6}Sr_{0.4}MnO_3$(LSM)	R3c R3c	5.507 5.490	5.507 5.490	13.255 13.356
Electrolyte $BaCe_{0.89}Gd_{0.1}Cu_{0.01}O_3$(BCGCu) $Ce_{0.8}Sm_{0.2}O_{1.9}$(SDC)	 Pmcn Fm3m	 8.791 5.437	 6.252 -	 6.218 -

Table 2
Phase composition of La_2NiO_4-based functional electrode layers after sintering at 1200 °C and after holding at 700 °C during 1000 h (XRD data)

Electrode composition before sintering	Phase composition after sintering	Phase composition after 1000 h
LCNO-BCGCu $BaCe_{0.9}Gd_{0.1}O_{2.95}$ $La_{1.7}Ca_{0.3}NiO_4$	$BaCe_{0.9}Gd_{0.1}O_{2.95}$ $La_{1.7}Ca_{0.3}NiO_4$ BaO	$Ce_{0.9}Ca_{0.1}O_{1.9}$ $La_{1.7}Ca_{0.3}NiO_4$ $BaCe_{0.9}Gd_{0.1}O_{2.95}$ $Ba_2Cu_3O_x$
LSNO-BCGCu $BaCe_{0.9}Gd_{0.1}O_{2.95}$ $La_{1.7}Sr_{0.3}NiO_4$	$BaCe_{0.9}Gd_{0.1}O_{2.95}$ $La_{1.71}Sr_{0.19}NiO_{3.9}$ BaO $Ba_2Cu_3O_x$	$BaCe_{0.9}Gd_{0.1}O_{2.95}$ $La_{1.7}1Sr_{0.19}NiO_{3.9}$ BaO $Ba_2Cu_3O_x$
LBNO-BCGCu $BaCe_{0.9}Gd_{0.1}O_{2.95}$ $La_{1.52}Ba_{0.48}NiO_4$	$BaCe_{0.9}Gd_{0.1}O_{2.95}$ $La_{1.52}Ba_{0.48}NiO_4$ $BaNi_4O_8$ $La_2NiO_{4.1}$	$BaCe_{0.9}Gd_{0.1}O_{2.95}$ $La_{1.52}Ba_{0.48}NiO_4$ BaO
LCNO-SDC $La_{1.7}Ca_{0.3}NiO_4$ $Sm_{0.2}Ce_{0.8}O_{1.9}$	$Sm_{0.2}Ce_{0.8}O_{1.9}$ $La_{1.7}Ca_{0.3}NiO_4$ $LaNiO_3$ $Ce_{11}O_{20}$	$Sm_{0.2}Ce_{0.8}O_{1.9}$ $La_{1.7}Ca_{0.3}NiO_4$ $LaNiO_3$ Sm_2O_3
LSNO-SDC $La_{1.7}Sr_{0.3}NiO_4$ $Sm_{0.2}Ce_{0.8}O_{1.9}$	$Sm_{0.2}Ce_{0.8}O_{1.9}$ $La_{1.7}1Sr_{0.19}NiO_{3.9}$ $Ce_{11}O_{20}$	$Sm_{0.2}Ce_{0.8}O_{1.9}$ $La_{1.7}1Sr_{0.19}NiO_{3.9}$ SrN_xO_z NiO $LaNiO_3$
LBNO-SDC $La_{1.52}Ba_{0.48}NiO_4$ $Sm_{0.2}Ce_{0.8}O_{1.9}$	$La_{1.7}Ba_{0.3}NiO_4$ $Sm_{0.2}Ce_{0.8}O_{1.9}$ $Ce_{11}O_{20}$	$Sm_{0.2}Ce_{0.8}O_{1.9}$ $BaOLa_2NiO_4$ $BaNiO_2$ NiO

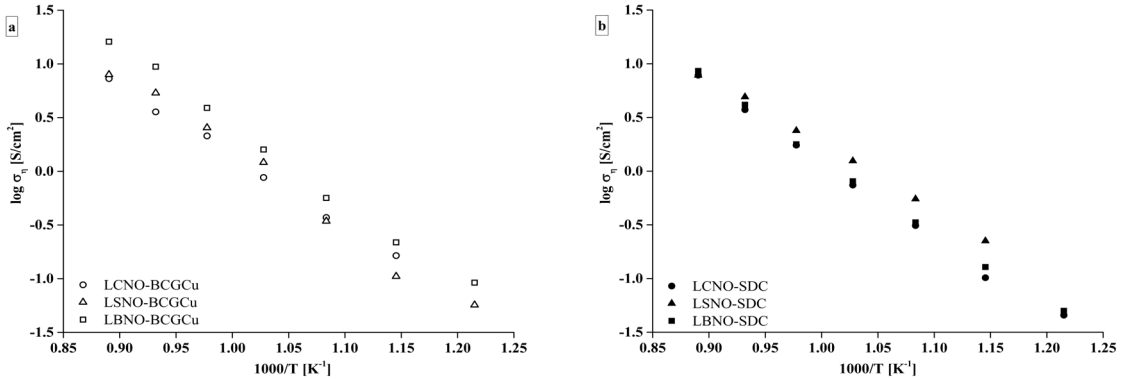

Fig. 2. Arrenius plots of the polarization conductivity of the bi-layered composite electrodes with BCGCu (a) and SDC (b) ceramic component.

Table 3

Polarization (R_η) and serial resistance (R_{hf}) of the composite electrodes measured after sintering (0 h) and after long-term testing (1500 h); energies of activation of polarization, serial conductivity and total conductivity in air for BCGCu electrolyte

Electrode composition	$R\eta_0$ [Ω cm^2]	$R\eta_{1500}$ [Ω cm^2]	$dR\eta_{1500}$ [%]	R_{hf0} [Ω cm]	dR_{hf1500} [%]	Ea_η [eV]	Ea_{hf} [eV]
LCNO-BCGCu	1.14	1.87	63.48	84.24	2.22	1.29	0.45
LSNO-BCGCu	0.73	0.68	-7.06	94.31	-0.04	1.60	0.46
LBNO-BCGCu	0.63	0.30	-53.02	73.69	5.95	1.42	0.42
LCNO-SDC	1.40	1.69	20.85	86.01	-1.72	1.39	0.46
LSNO-SDC	0.80	0.66	-1751	88.55	3.26	1.21	0.43
LBNO-SDC	1.28	1.44	13.12	90.31	11.38	1.37	0.44
BCGCu							0.47

Figure 2 a-b depict the temperature dependence of polarization conductivity of the investigated bi-layered electrodes with BCGCu and SDC ceramic component in their functional layer, respectively. The lowest values of polarization conductivity were found for the composites with Ca (0.74 and 0.88 S cm^{-2} at 700 °C, respectively). LCNO-SDC in contact with BCGCu electrolyte showed almost the same σ_η value as in contact with SDC electrolyte [21]. The composites with Sr showed high values of the polarization conductivity for both BCGCu and SDC ceramic component (1.25 and 1.21 S cm^{-2}, respectively). It should be noted, that in the case of Sr and Ca the composite electrodes with different ceramic components had almost the same values of polarization conductivity. Ba-substituted nickelate displayed diverse behaviour: if the characteristics of the LBNO-SDC were middling (Table 3) then the LBNO-BCGCu electrode showed both the highest σ_η and σ_{hf} values (1.59 S cm^{-2} and 13.57 × 10^{-3} S cm^{-2}). The highest value of the polarization conductivity of the composite electrode $L_2NiO_{4+\delta}$-$LaNi_{0.6}Fe_{0.4}O_{3-\delta}$ (70:30) measured on a symmetrical cell in contact with the proton-conducting electrolyte $BaZr_{0.1}Ce_{0.7}Y_{0.2}O_{3-\delta}$, presented in literature, is 0.47 S cm^{-2} (calculated from the data, presented in Table 2 in the recent work of J. Hou et al. [14]). All the developed electrodes in this work exhibited superior characteristics. Therefore, the experimental results reveal that fabrication of the bi-layered electrodes with a composite functional layer made of substituted LNO in a mixture with an ionic or co-ionic ceramic component and with an LNF collector layer is a feasible way to improve electrode characteristics.

The specific serial resistance of the cells with the composite electrodes studied is the highest for LSNO-BCGCu (Table 3, Fig. 3). It is most probably connected with the strong interaction between the components in the composite material. The close agreement in the values of the activation energies of the reciprocal serial resistance of the electrodes (0.42–0.46 eV) and the total conductivity of the BCGCu electrolyte (0.47 eV) suggests that the serial resistance is determined, mainly, by the resistance of the electrolyte support.

The long-term tests showed that serial resistance of all the electrodes investigated decreased during the first 500 h with subsequent total growth no more than 11% of the initial value (Table 3, Fig. 4 a). Polarization resistance of both composite electrodes with Ca-substituted nickelate increased dramatically during testing and in fact, the greatest changes took place during the first 500 h (Fig. 4 b, c). The LBNO-SDC composite electrode showed moderate changes while the polarization resistance of LBNO-BCGCu, LSNO-SDC and LSNO-BCG-Cu decreased with time.

Figure 5 shows the spectra of the composite electrodes before and after long-term testing. All the measured spectra were asymmetric in shape, implying more than one electrode process. Usually for the description of spectra of LNO-based electrodes the equivalent circuits containing two [14, 25] or three distributed elements [26], composed of a constant phase element (*Q*) in parallel with a resistance (*R*) are used. The equivalent capacitance C and relaxation frequency f of an electrode process corresponding to a specific (*RQ*) can be applied as characteristic parameters to identify various electrode processes. The high-frequency electrode processes with the effective capacitances of approximately 10^{-6}–10^{-5} F cm^{-2} have been associated with the transport of oxygen ions across the interface between the electrode and electrolyte. In the middle frequency range the processes with the effective capacitances of 10^{-4}–10^{-3} is assigned to the diffusion of oxygen ions into the electrode volume accompanied by a charge transfer, while in the low-frequency range the processes with the effective capacitances of 10^{-3}–10^{-1} is ascribed to the adsorption and dissociation of the molecular oxygen on the electrode surface [26].

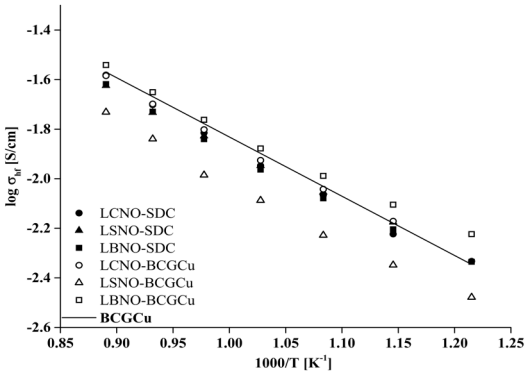

Fig. 3. Arrenius plots of the reciprocal serial resistance of the bi-layered composite electrodes.

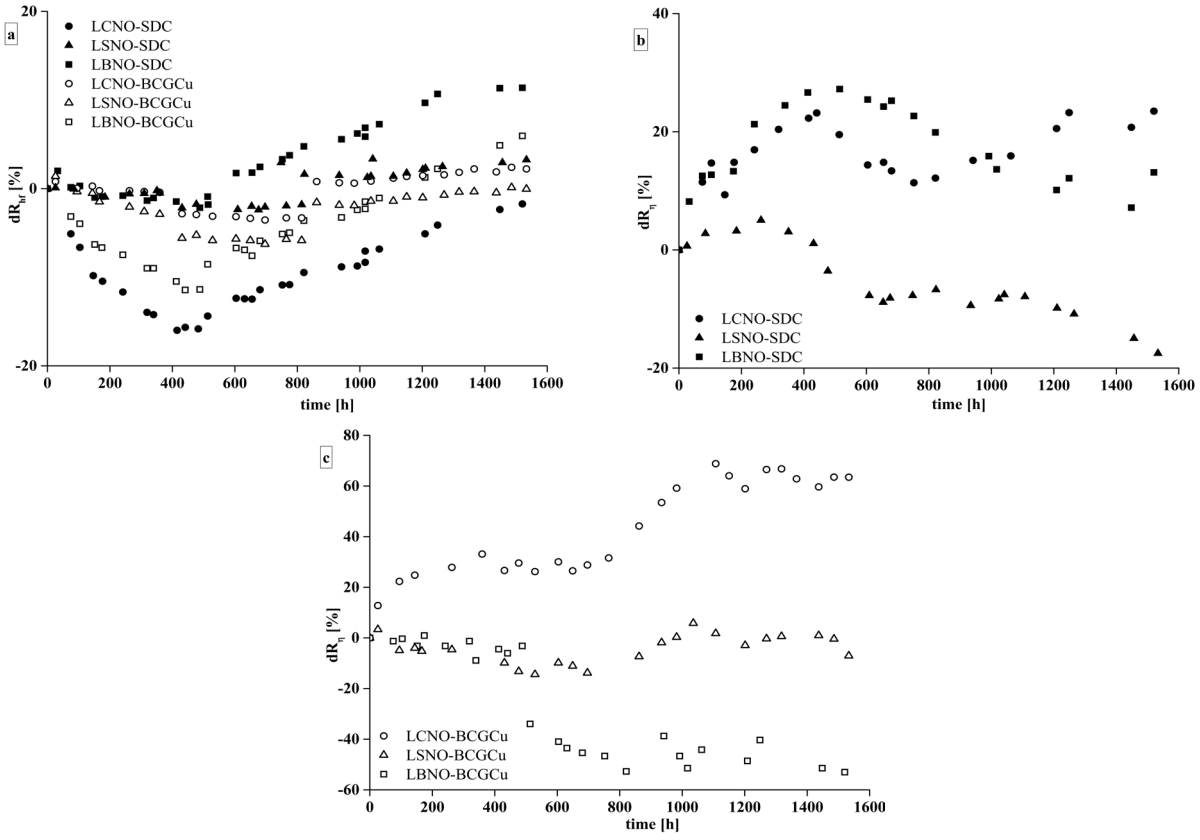

Fig. 4. Relative change in the serial resistance (a) and polarization resistance (b, c) of the bi-layered composite electrodes in long-term testing at 700 °C.

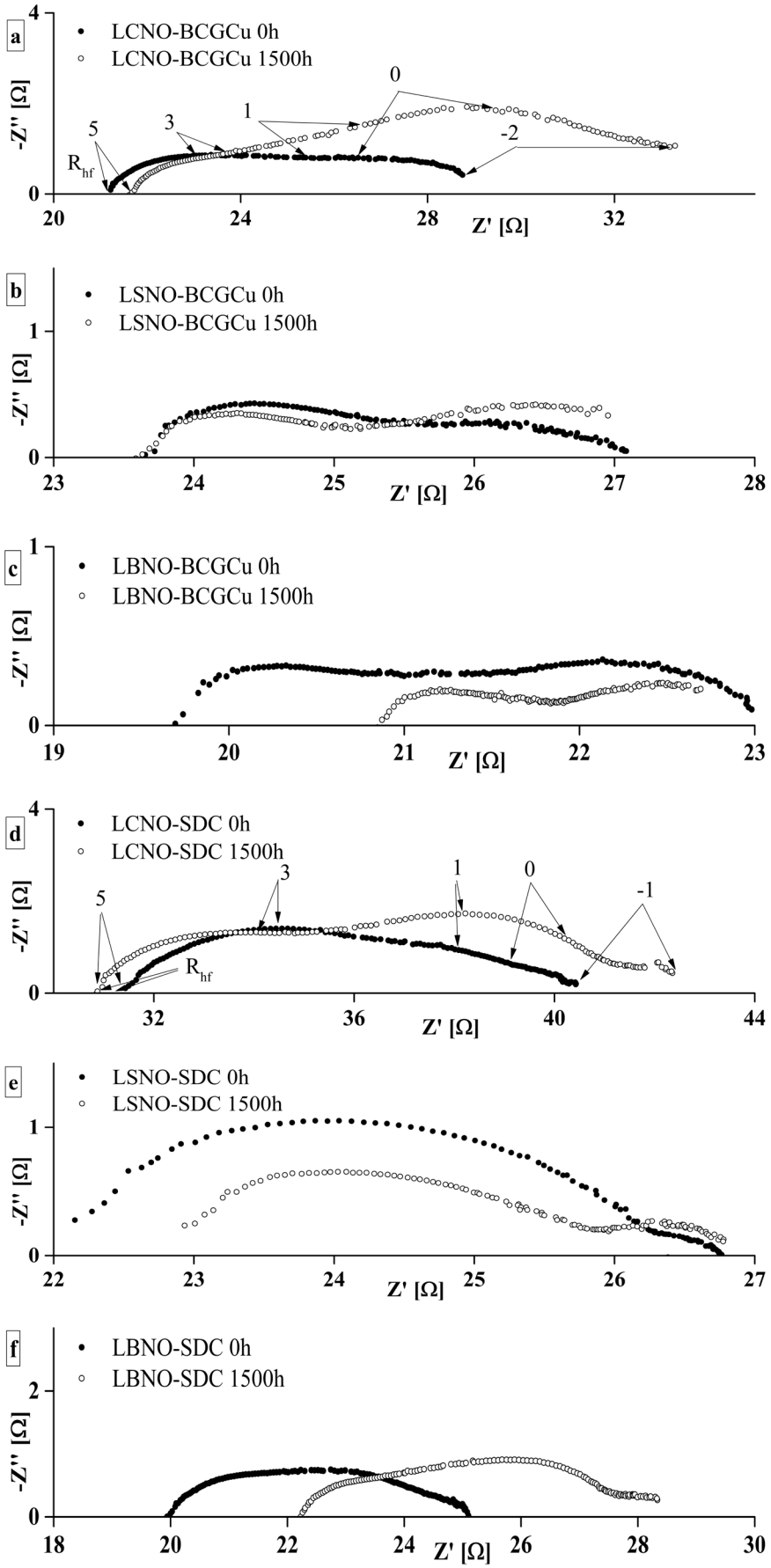

Fig. 5. Nyquist plots of the impedance spectra measured before (closed symbols) and after (opened symbols) long-term testing for the composite electrodes with BCGCu (a, b, c) and SDC (e, f, g) ceramic component.

According to an estimation of the contribution of the high- and low-frequency processes in the total polarization resistance by the analysis of the spectra before and after 1500 h of testing the following features were found: the capacitance and resistance of the high-frequency process for LCNO-BCGCu did not change with time, while the capacitance of the low-frequency reduced by the order of magnitude and the resistance grew from 4.89 to 8.6 Ω (Fig. 5 a). For LCNO-SDC the capacitance and resistance of the high-frequency process did not show significant changes as well, where as the capacitance of the low-frequency process increased by the order of magnitude and its resistance grew from 2.46 to 6.66 Ω (Fig. 5 d). Such serious changes in spectra seemed to appear due to the strong interaction of the components of the composite electrodes based on LCNO, as was mentioned above (Table 2).

LSNO-BCGCu and LSNO-SDC (Fig. 5 b, e) showed polarization characteristics stable in time. The resistance of high-frequency processes slightly decreased with time with simultaneous small increasing the resistance of the electrode processes in the middle and low frequency ranges. Similarly to the electrodes based on Ca-substituted nickelate these changes are related to the chemical interaction between the electrode components but for Sr-substituted nickelate the interaction is lower. The main feature of both electrodes based on Ba-substituted nickelates (Fig. 5 c, f) and LSNO-SDC (Fig. 5 e) is a significant increase in the serial resistance R_{hf}. As far as the shape of the high-frequency region of spectra did not change during long-term testing, an increase in the serial resistance may be related to incompatibility in CTE for some composite electrodes and BCGCu electrolyte. To verify this assumption the temperature dependences of linear expansion of the electrolyte and electrode materials under investigation were measured and the CTE values of the composite materials were calculated as an arithmetic mean value of the individual components. The CTE value of the BCGCu electrolyte changes from 10.5×10^{-6} K^{-1} in the temperature range 100–575 °C to 8.6×10^{-6} K^{-1} in the temperature range 575–900 °C, respectively, the CTE value of the SDC electrolyte in the temperature range 100–900 °C is 12.5×10^{-6} K^{-1}. The individual CTE values of the LCNO, LSNO and LBNO electrode materials are 13.9, 14.2 and 15.2 $\times 10^{-6}$ K^{-1}, respectively. The CTE values of the composites with BCGCu and SDC are 11.3–11.9, 11.4–12.4, 11.9–12.9 $\times 10^{-6}$ K^{-1} and 13.2, 13.4, 13.9 $\times 10^{-6}$ K^{-1}, respectively. Despite having adequate adhesion during sintering a difference of more than 30% in CTE leads to partial delamination of the electrode, increasing the serial resistance.

It should be noted that in contrast to the LBNO-SDC electrode, which showed an increase both in serial and total resistance (Fig. 5 f), the total resistance of the LBNO-BCGCu electrode remained almost constant with time. Besides the polarization resistance of the LBNO-BCGCu electrode decreased by approximately a factor of two and reached 0.30 Ω · cm^2 after the long-term testing.

4. Conclusions

This work aimed to study the influence of the substituting element in the bi-layered $La_{1.7}M_{0.3}NiO_{4+\delta}$–based (M = Ca, Sr, Ba) composite cathodes with $BaCe_{0.89}Gd_{0.1}Cu_{0.01}O_3$ or $Ce_{0.8}Sm_{0.2}O_{2-\delta}$ ceramic component on their electrochemical behavior in contact with $BaCe_{0.89}Gd_{0.1}Cu_{0.01}O_3$ proton-conducting electrolyte. The best characteristics (the lowest value of the polarization resistance in combination with low serial resistance) were found for the electrode with $La_{1.7}Ba_{0.3}NiO_{4+\delta}$ – $BaCe_{0.89}Gd_{0.1}Cu_{0.01}O_3$ functional layer and 99.4 wt.% $La_{0.6}Sr_{0.4}MnO_3$ + 0.6 wt.% CuO collector (0.63 Ω cm^2 and 73.69 Ω cm at 700 °C, respectively). After 1500 h of high temperature testing and 2 thermo-cycles the polarization resistance of the developed electrode reduced to 0.30 Ω cm^2.

Acknowledgments

This work was partly done using facilities of the shared access center “Composition of compounds” IHTE, UB RAS. The authors are grateful to N.M. Bogdanovich and T.A. Dem’yanenko (IHTE UB RAS) for the sample preparation, I.V. Nikolaenko (ISSC, UB RAS) f or the microstructure investigations and S.V. Plaksin (IHTE UB RAS) for the XRD testing. We very thank Prof. Dimitry Bronin (IHTE UB RAS), Mr. Peter Roy Orman (BA Victoria University of Wellington, New Zealand) for the manuscript proof-reading. The research was financially supported by the Program of UD RAS (project No 15-20-3-15), the Russian Foundation for Basic Research (grants No 14-03-00414, 16-33-00883) and by Act 211 Government of the Russian Federation, contract № 02.A03.21.0006.

References

[1]. D.A. Medvedev, J.G. Lyagaeva, E.V. Gorbova, A.K. Demin, and P. Tsiakaras, Prog. Mater. Sci. 75 (2016) 38–79.

[2]. D.A. Medvedev, E.V. Gorbova, A.K. Demin, and P. Tsiakaras, Int. J. Hydrog. Energy 39 (2014) 21547–21552.
[3]. A. Demin, P. Tsiakaras, Int. J. Hydrog. Energy 26 (2001) 1103–1108
[4]. V. Menon, A. Banerjee, J. Dailly, and O. Deutschmann, Appl. Energy 149 (2015) 161–175.
[5]. Y.-P. Fu, Ch.-S. Weng, Ceram. Int. 40 (2014) 10793−10802.
[6]. M. Ananyev, D. Medvedev, A. Gavrilyuk, M. Stratigoula, A. Demin, V. Malkov, and P. Tsiakaras, Electrochem. Acta 125 (2014) 371−379.
[7]. D. Medvedev, A. Murashkina, E. Pikalova, A. Demin, A. Podias, and P. Tsiakaras, Prog. Mater. Sci. 60 (2014) 72–129.
[8]. E.V. Tsipis, V.V. Kharton, J. Solid State Electrochem. 12 (2008) 1039–1060.
[9]. D. Poetzsch, R. Merkle, and J. Maier, J. Eletrochem. Soc. 162 (2015) F939-F950.
[10]. P.-M. Geffroy, M. Reichmann, T. Chartier, J.-M. Bassat, and J.-C. Grenier, J. Membr. Sci. 451 (2014) 234–242.
[11]. C. Laberty, F. Zhao, K.E. Swider-Lyons, and A.V. Virkar, Electrochem. Solid-State Lett. 10 (2007) B170–B174.
[12]. J. Dailly, S. Fourcade, A. Largeteau, F. Mauvy, J.C. Grenier, and M. Marrony, Electrochem. Acta 55 (2010) 5847–5853.
[13]. C. Solis, L. Navarrete, and J.M. Serra, J. Power Sources 240 (2013) 691–697.
[14]. J. Hou, Zh. Zhiwen, J. Qian, and W. Liu, J. Power Sources 264 (2014) 67–75.
[15]. J.P. Tang, R.I. Dass, and A. Manthiram, Mater. Res. Bull. 35 (2000) 411–424.
[16]. Y. Shen, H. Zhao, X. Liu, and N. Xu, Phys. Chem. Chem. Phys. 12 (2010) 15124–15131.
[17]. E.Yu. Pikalova, N.M. Bogdanovich, A.A. Kolchugin, D.A. Osinkin, and D.I. Bronin, Procedia Engineering 98 (2014) 105–110.
[18]. L.-P. Sun, Q. Li, H. Zhao, L.-H. Huo, and J.-C. Grenier, J. Power Sources 183 (2008) 43–48.
[19]. S. Simeonov, S. Kozhukharov, J.-C. Grenier, M. Machkova, and V. Kozhukharov, J. Chem. Technol. Metallurgy 48 (2013) 104–110.
[20]. S.S. Bhoga, A.P. Khandale, and B.S. Pahunde, Solid State Ionics 262 (2014) 340–344.
[21]. E.Yu. Pikalova, A.A. Kolchugin, N.M. Bogdanovich, and D.I. Bronin, Adv. Sci. Technol. 93 (2014) 25–30.
[22]. E. Gorbova, V. Maragou, D. Medvedev, A. Demin, and P. Tsiakaras, J. Power Sources 181 (2009) 292–296.
[23]. I.Yu. Yaroslavtsev, B.L. Kuzin, D.I. Bronin, G.K. Vdovin, N. Bogdanovich, Rus. J. Electrochem. 45 (2007) 875–880.
[24]. M. Mogensen, N.M. Sammes, and G.A. Tompsett, Solid State Ionics 129 (2000) 63–94.
[25]. K. Zhao, Y.-P. Wang, M. Chen, Q. Xu, B.-H. Kim, and D.-P. Huang, Int. J. Hydrog. Energy 39 (2014) 7120–7130.
[26]. K. Zhao, Q. Xu, D.-P. Huang, M. Chen, and B.-H. Kim, Ionics 18 (2012) 75–83.